Mechanism of Reoxygenation after Antiangiogenic Therapy Using SU5416 and Its Importance for Guiding Combined Antitumor Therapy

Réginald Ansiaux,[1] Christine Baudelet,[1,2] Bénédicte F. Jordan,[1,2] Nathalie Crokart,[1] Philippe Martinive,[3] Julie DeWever,[3] Vincent Grégoire,[4] Olivier Feron,[3] and Bernard Gallez[1,2]

[1]Laboratory of Biomedical Magnetic Resonance, [2]Laboratory of Medicinal Chemistry and Radiopharmacy, [3]Laboratory of Pharmacology and Therapeutics, and [4]Laboratory of Molecular Imaging and Experimental Radiotherapy, Université Catholique de Louvain, Brussels, Belgium

Abstract

Emerging preclinical studies support the concept of a transient "normalization" of tumor vasculature during the early stage of antiangiogenic treatment, with possible beneficial effects on associated radiotherapy or chemotherapy. One key issue in this area of research is to determine whether this feature is common to all antiangiogenic drugs and whether the phenomenon occurs in all types of tumors. In the present study, we characterized the evolution of the tumor oxygenation (in transplantable liver tumor and FSAII tumor models) after administration of SU5416, an antagonist of the vascular endothelial growth factor receptor. SU5416 induced an early increase in tumor oxygenation [measured by electronic paramagnetic resonance (EPR)], which did not correlate with remodeling of the tumor vasculature (assessed by CD31 labeling using immunohistochemistry) or with tumor perfusion (measured by dynamic contrast enhanced-magnetic resonance imaging). Inhibition of mitochondrial respiration (measured by EPR) was responsible for this early reoxygenation. Consistent with these unique findings in the tumor microenvironment, we found that SU5416 potentiated tumor response to radiotherapy but not to chemotherapy. In addition to the fact that the characterization of the tumor oxygenation is essential to enable correct application of combined therapies, our results show that the long-term inhibition of oxygen consumption is a potential novel target in this class of compounds. (Cancer Res 2006; 66(19): 9698-704)

Introduction

Tumor angiogenesis is a complex and multistep process involving different angiogenic factors and allowing tumors to grow and metastasize. The resulting tumor vascular bed presents structural abnormalities. Blood vessels are disorganized, poorly connected, tortuous, leaky, and irregularly shaped with areas of dilation and constriction. Endothelial cell arrangement is abnormal: no tight junctions and absent or abnormal pericytes and basal membrane. The net result is a vascular network that is spatially and temporally heterogeneous, leading to an abnormal tumor microenvironment characterized by chaotic perfusion, hypoxic zones, acidosis, and high interstitial fluid pressure (1).

The widely accepted mechanism of action of antiangiogenic drugs is that they prevent the formation of these new tumor blood vessels, thus inhibiting tumor growth (2, 3). In addition to this long-term "starvation" effect of antiangiogenic therapy, recent preclinical studies support the concept of a transient normalization of the tumor vasculature (1) during the early stage of antiangiogenic treatment (4–11). This concept, first proposed by Jain (1), suggests that antiangiogenic agents first prune the immature and inefficient blood vessels and then induce a remodeling of the remaining vasculature, leading to a transiently improved tumor vasculature (1, 12). This phenomenon results in a transient increase in tumor perfusion and a reoxygenation of the tumor. The resultant increase in delivery of drugs and oxygen into the tumor enhances the actions of chemotherapy and radiotherapy, as shown in previous studies using thalidomide (5, 11), a drug that acts on vascular endothelial growth factor (VEGF) and basic fibroblast growth factor (bFGF) signaling. With the advent of several classes of antiangiogenic agents, oncologists will be able to choose among new potent drugs. To properly design therapy protocols, especially those that combine antiangiogenic agents with radiotherapy or chemotherapy, several key questions need to be answered: (*a*) do all antiangiogenic agents produce a transient normalization of tumor vasculature?; (*b*) which tumor hemodynamic variables are affected?; (*c*) what are the kinetics in the evolution of the tumor oxygenation?; and (*d*) what are the consequences for the effects of combined therapies?

In the present study, our attention focused on the evolution of the tumor oxygenation after administration of SU5416, an antiangiogenic agent that binds to the VEGF receptor (VEGFR), Flk-1/KDR, thereby inhibiting the action of VEGF (13, 14). We report the unique finding that SU5416 induced early tumor reoxygenation, which was associated with an inhibition of mitochondrial respiration but not with any effect on tumor perfusion. Unraveling the mechanisms at the origin of the reoxygenation (balance between tumor oxygen supply and tumor cell oxygen consumption) provides an essential marker of the effects of treatment with combined therapies. A significant benefit was observed with the association of SU5416 and radiotherapy, a fact that is consistent with reoxygenation of the tumor. However, no benefit was found from the association of SU5416 and chemotherapy using cyclophosphamide, which is consistent with the lack of effect on tumor perfusion. In addition to the fact that characterization of the tumor oxygenation is essential to enable combined therapies to be applied correctly, our results show that the inhibition of oxygen consumption is a potential novel target in this class of compounds.

Note: R. Ansiaux is a National Fund for Scientific Research (FNRS)-Televie fellow; C. Baudelet and B.F. Jordan are Scientific Research workers of the FNRS; and O. Feron is a Research Associate of the FNRS.

Requests for reprints: Bernard Gallez, CMFA/REMA Units, Université Catholique de Louvain, Avenue E. Mounier 73.40, B-1200 Brussels, Belgium. Phone: 32-2-7642792; Fax: 32-2-7642790; E-mail: Gallez@cmfa.ucl.ac.be.

doi:10.1158/0008-5472.CAN-06-1854

Materials and Methods

Mice and Tumor Models

Two different tumor models were implanted in the thighs of mice: a transplantable mouse liver tumor (TLT) model (15) in NMRI mice and a syngeneic FSAII fibrosarcoma model (16) in C3H/HeOuJIco mice. Tumor size was measured daily with an electronic caliper. For all experiments, tumor-bearing mice were anesthetized using isoflurane (3% for induction; 1.5% for maintenance). To maintain normothermia, mice were placed on a heating pad (37°C) for all experiments, except for the dynamic contrast enhanced (DCE)–magnetic resonance imaging (MRI) where warm air was flushed into the magnet. All animal experiments were conducted in accordance with national animal care regulations. These tumor models were chosen because the antiangiogenic agent, thalidomide, caused early normalization of their tumor vasculature (5, 11).

Treatments

SU5416 was purchased from Sigma-Aldrich (Bornem, Belgium). For the treated group, SU5416 was dissolved in DMSO (Sigma-Aldrich) and given i.p. at a dose of 25 mg/kg body weight once a day via a 100-μL injection. Control animals were treated with DMSO only. The daily antiangiogenic therapy was started when tumors reached a diameter of 7.5 ± 0.5 mm, which corresponds to ~7 days after tumor inoculation.

Tumor Oxygenation

Electronic paramagnetic resonance (EPR) oximetry, using charcoal (CX0670-1; EM Science, Gibbstown, NJ) as the oxygen-sensitive probe, was used to evaluate changes in tumor oxygenation after treatment with SU5416, using a protocol described previously (17). EPR spectra were recorded using an EPR spectrometer (Magnettech, Berlin, Germany) with a low frequency microwave bridge operating at 1.2 GHz and an extended loop resonator. A suspension of charcoal was injected via a 26-gauge needle in the center of the tumor 1 day before measurement (100 mg/mL; 50 μL injected; particle size of 1-25 μm). The localized EPR measurements correspond to an average of pO_2 values in a volume of ~10 mm^3 (17). To avoid any acute effect of the treatment, data acquisition was done before the injection of SU5416 or DMSO and then on a daily basis for 1 week. The acute effect of SU5416 was also measured by following the tumor pO_2 status for 1 hour after the single injection. Three measurements were acquired as a baseline before the injection.

Flow Measurements

Patent blue staining. Patent blue (Sigma-Aldrich) was used to obtain a rough estimate of tumor perfusion (5) 24 hours after the second injection of treatment with SU5416 or DMSO. This technique involves the injection of 200 μL patent blue (1.25%) solution into the tail vein of the mice. After 1 minute, uniform distribution of stain was obtained through the body and the mice were sacrificed. The tumors were carefully excised and cut into two size-matched halves. Pictures of each tumor cross-section were taken with a digital camera. To compare the stained versus unstained areas, an in-house program running on Interactive Data Language (RSI, Boulder, CO) was developed. For each tumor, a region of interest (stained area) was defined on the two pictures and the stained percentage of the whole cross-section was determined. The mean of the percentages of the two pictures was then calculated and used as an indicator of tumor perfusion.

DCE-MRI. This technique was used to assess changes in tumor perfusion and permeability 24 hours after the second SU5416 or DMSO injections. Single-slice dynamic contrast-enhanced MRI was done with a 4.7 T (200 MHz, ^1H) 40 cm inner diameter bore system (Bruker Biospec, Ettlingen, Germany) using the rapid-clearance blood pool agent, P792 (Vistarem, Guerbet, Roissy, France; ref. 18). High-resolution multislice T_2-weighed spin echo anatomic imaging was done just before dynamic contrast-enhanced imaging. Pixel-by-pixel values for K^{trans} (influx volume transfer constant, from plasma into the interstitial space, units of $minute^{-1}$), V_p (blood plasma volume per unit volume of tissue, unitless), and K_{ep} (fractional rate of efflux from the interstitial space back to blood, units of $minute^{-1}$) in the tumor were calculated via tracer kinetic modeling of the dynamic contrast-enhanced data (18), and the resulting parametric maps for K^{trans}, V_p, and K_{ep} were generated. Statistical significance for V_p or K^{trans} identified "perfused" pixels (i.e., pixels to which the contrast agent P792 had access; refs. 18, 19).

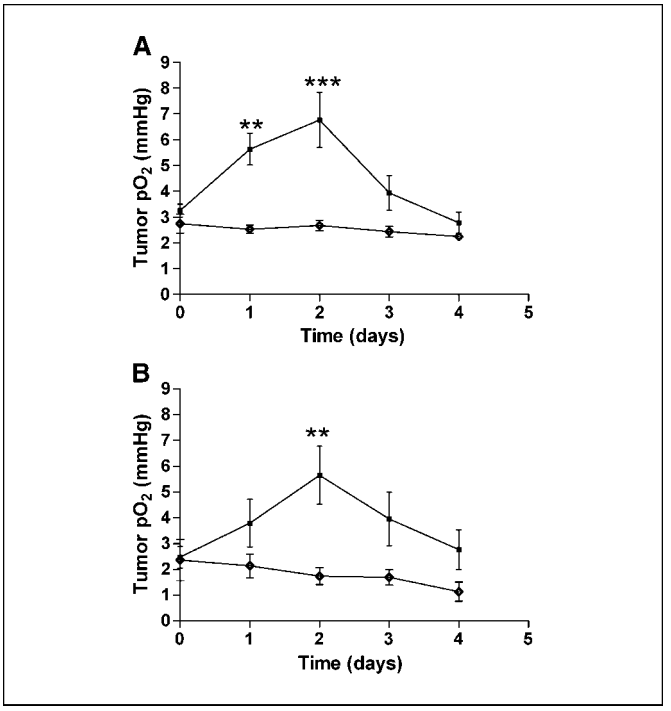

Figure 1. Effect of daily SU5416 injection on TLT tumor (*A*) and FSAII tumor (*B*) oxygenation monitored by EPR oximetry. ◇, control group (n = 4 for TLT and FSAII); ■, treated group (n = 6 and n = 4 for TLT and FSAII, respectively). Note the significant increase in pO_2 24 hours after the first injection, with a maximum on day 2. *Points,* mean; *bars,* SE. **, $P < 0.01$; ***, $P < 0.001$.

Oxygen Consumption Rate Evaluation

The method used by Jordan et al. (20) was used. All spectra were recorded on a Bruker EMX EPR spectrometer operating at 9 GHz. TLT tumor-bearing mice were treated for 2 days with SU5416 at a dose of 25 mg/kg via 100-μL i.p injection. Twenty-four hours after the second injection, the mice were sacrificed and the tumor was excised. TLT tumors were then dissected in a sterile environment and gently pieced in McCoy's medium. The cell suspension was trypsinized before being filtered (100-μm pore nylon filter; Millipore, Brussels, Belgium) and centrifuged (5 minutes; 1,500 t/min; 4°C). Then, cell viability was determined. Cells were suspended in 10% dextran in complete medium A neutral nitroxide, ^{15}N 4-oxo-2,2,6,6-tetramethylpiperidine-d_{16}-^{15}N-1-oxyl at 0.2 mmol/L (CDN Isotopes, Pointe-Claire, Quebec, Canada), was added to 100 μL aliquots of tumor cells that were then drawn into glass capillary tubes. The probe (0.2 mmol/L in 20% dextran in complete medium) was calibrated at various O_2 concentrations between 100% nitrogen and air so that the line width measurements could be related to O_2 concentration at any value. Nitrogen and air were mixed in an Aalborg gas mixer, and the oxygen concentration was analyzed using a Servomex (Hamm, Germany) oxygen analyzer OA540. The sealed tubes were placed into quartz EPR tubes, and samples were maintained at 37°C. As the resulting line width reports on O_2 concentration, oxygen consumption rates were obtained by measuring the O_2 concentration in the closed tube over time and finding the slope of the resulting linear plot.

Radiation Sensitivity *In vivo*

The TLT tumor-bearing leg was irradiated locally with 10 Gy of 250 kV X-rays (RT 250; Philips Medical Systems, Hamburg, Germany). The tumor was centered in a circular irradiation field measuring 3 cm in diameter.

A single-dose irradiation of 10 Gy was given 24 hours after the second injection of SU5416 treatment. After radiotherapy, tumor growth was determined daily by measuring transverse and antero-posterior tumor diameters until they reached 18 mm, at which time the mice were sacrificed. A linear fit was done between 8 and 16 mm, which allowed determination of the time to reach a particular size (tumor measuring 12 mm in diameter) for each mouse.

Radiation Sensitivity *In vitro*

TLT tumors in mice were dissected in a sterile environment and gently pieced in McCoy's medium. The cell suspension was filtered (100-μm pore nylon filter) and centrifuged (5 minutes; 450 g; 4°C), and cells were set to culture in DMEM containing 10% fetal bovine serum. Confluent cells were treated with SU5416 (25 μmol/L) 2 hours before being irradiated at 2 Gy. To assess the cell radiosensitivity, the trypan blue exclusion dye method was done: cells were counted for viability 24 hours after irradiation. The experiments were carried out in triplicate. It should be noted that the classic clonogenic assay was impossible using this model because colonies could not form.

Chemotherapy Sensitivity

SU5416-treated mice (2 days) received a single dose (50 mg/kg via 100 μL i.p. injection) of cyclophosphamide, an alkylating agent. Regrowth delay experiments with TLT have shown that this dose of 50 mg/kg is just below the efficacy threshold for this product (experiments done with doses of 250-10 mg/kg).

Immunochemistry

TLT tumor-bearing mice were sacrificed after 2 days of treatment with SU5416 or DMSO. Tumor cryoslices were immunoprobed with rat monoclonal CD31 IgG2a antibodies (PharMingen, San Diego, CA). Rabbit polyclonal anti-rat IgG peroxidase-conjugated antibodies (Jackson ImmunoResearch Laboratories, West Grove, PA) and amino-ethyl-carbazole substrate system (DakoCytomation, Heverlee, Belgium) were used for revelation; sections were then counterstained with Mayer's hematoxylin.

Statistical Analysis

Results are given as mean ± SE values from n animals. Comparisons between groups were made with Student's two-tailed t test or two-way ANOVA where appropriate, and a $P < 0.05$ was considered significant.

Results

Effect of SU5416 on tumor oxygenation. EPR oximetry is designed for continuous measurement of the local pO_2 without altering the local oxygen concentration and allows repeated, real-time measurements from the same tissue over long periods (17). Initial TLT pO_2 have been measured on day 0 (before any treatment) and was found similar in both groups: SU5416 group, 3.2 ± 0.3 mm Hg (n = 6); control group, 2.7 ± 0.4 mm Hg

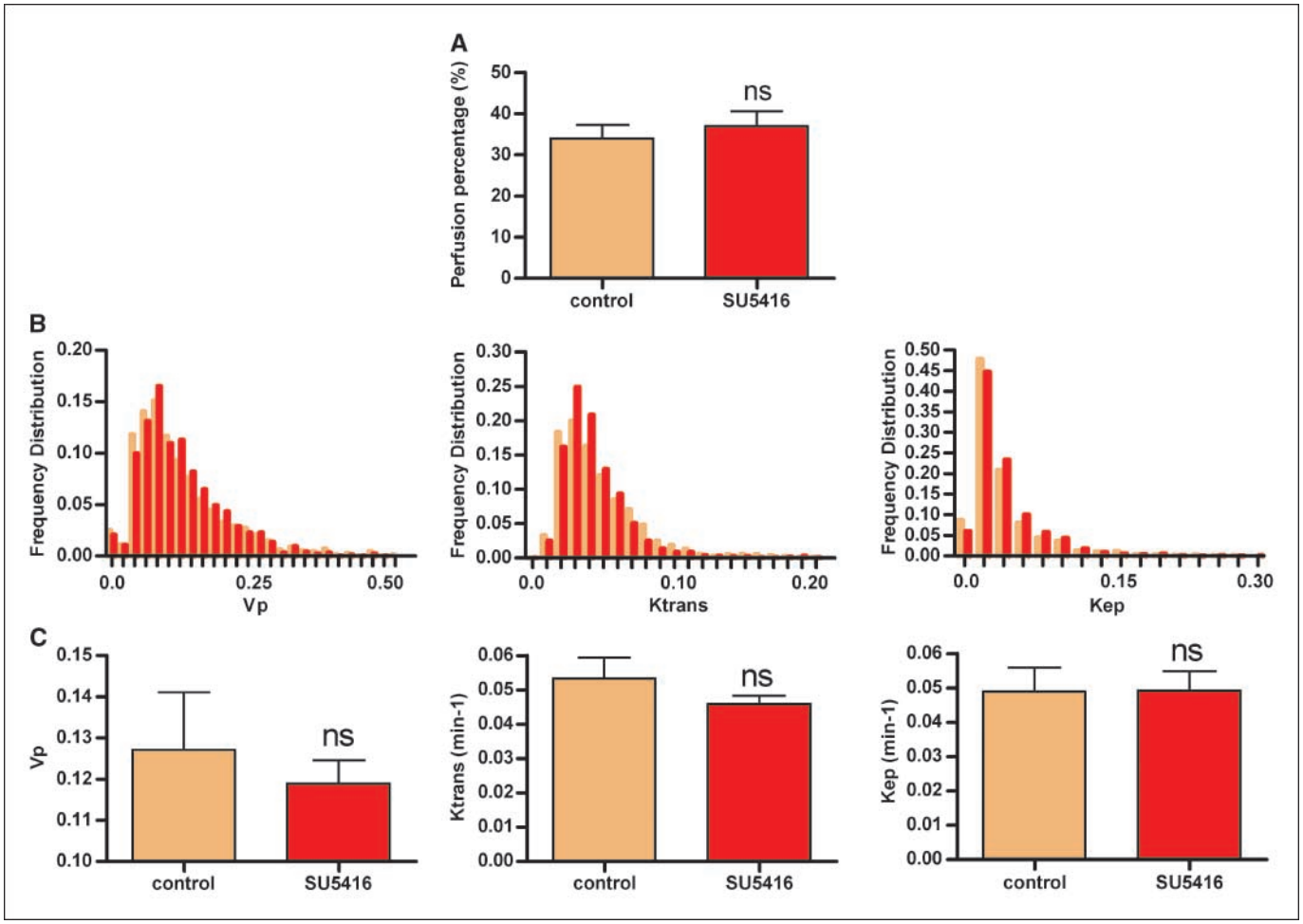

Figure 2. *A,* mean percentage of perfused pixels for treated (n = 5) and control group (n = 7). *B,* distribution of vascular variables in tumors treated with DMSO or SU5416. V_p is the blood plasma volume per unit volume of tissue, K^{trans} is the influx volume transfer constant from plasma into the interstitial space, and K_{ep} is the efflux volume transfer constant from the interstitial space back to the plasma. *C,* overall estimation of pharmacokinetic variables after SU5416 treatment. *Columns,* mean; *bars,* SE. *ns,* not significant.

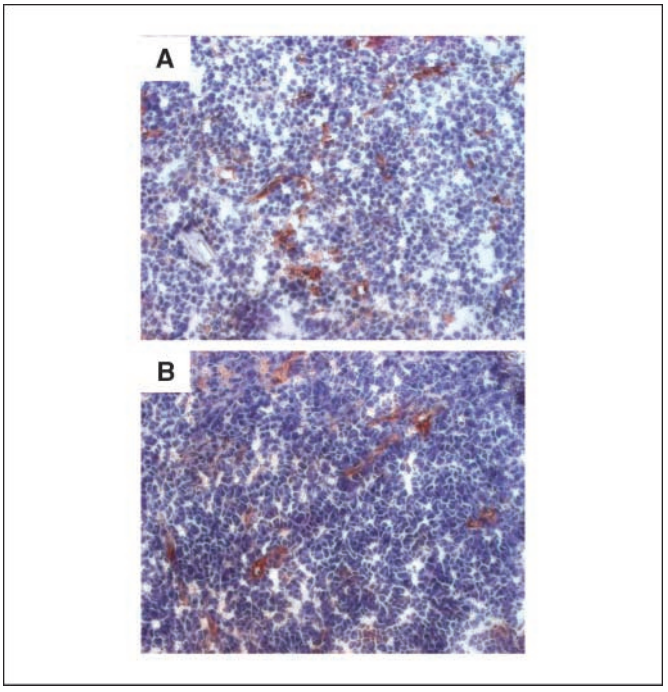

Figure 3. Typical histologic sections of TLT tumor after 2 days of treatment with SU5416 or DMSO. Immunohistologic staining was carried out with antibody against CD31. For both groups (*A*, control; *B*, treated), the vessels are evenly distributed throughout the tumor even in the center. No differences in the number of vessels, in dilation, or in necrosis were observed between groups.

(n = 4). Daily SU5416 injections significantly modified tumor pO_2 (Fig. 1*A*). For the treated group, tumor oxygenation increased after the first administration of SU5416 to reach a maximum after 2 days (6.8 ± 1.1 mm Hg) followed by a continuous decrease in pO_2. No such pO_2 increase was observed for the control group, in which values of pO_2 slowly decreased. Tumor pO_2 was statistically different between SU5416-treated tumors and controls (two-way ANOVA). The same effect was observed in FSAII tumors (Fig. 1*B*). All further experiments for the tumor characterization and determination of the therapeutic relevance of treatment with SU5416 were conducted on day 2, the time of maximal reoxygenation, on TLT tumors. We also found that the administration of SU5416 did not induce any changes in tumor pO_2 during the first hour after administration (data not shown).

Effects of SU5416 on tumor perfusion. Tumor perfusion was monitored in the TLT tumor model 24 hours after the second injection of SU5416 via dynamic contrast-enhanced MRI at 4.7 T using i.v. injection of the rapid-clearance blood pool agent P792 (Vistarem; ref. 18). The pixel-by-pixel analysis generated "perfusion maps" (using the values for V_p, the blood plasma volume per unit volume of tissue) and "permeability maps" (using the values for K^{trans}, the influx volume transfer constant, from plasma into the interstitial space, and K_{ep}, the efflux volume transfer constant from the interstitial space back to plasma). Moreover, the kinetic analysis identified "perfused pixels" (i.e., pixels to which the contrast agent had access, showing a statistical significance for V_p or K^{trans}; ref. 18). The fraction of perfused pixels for the tumors treated with SU5416 (Fig. 2*A*) was not significantly different than that of controls [36.94 ± 3.68% (n = 5) versus 33.96 ± 3.18% (n = 7), respectively; $P > 0.05$, Student's t test]. No differences in the average values of K^{trans}, K_{ep}, or V_p were observed between tumors treated with SU5416 or DMSO (Fig. 2*B* and *C*). These results indicate that SU5416 did not change tumor perfusion variables at this time of treatment. These results were further confirmed by a simple experiment where a rough estimate of tumor perfusion was carried out using the colored area observed in tumors 1 minute after i.v. injection of a dye (patent blue). No difference was observed between the treated and control groups [36.3 ± 1.9% (n = 4) for the SU5416 group and 30.16 ± 2.1% (n = 5) for controls].

Histologic analysis. Immunohistologic staining with antibody directed against CD31 was used to investigate whether tumor vascularization and organization were modified 2 days after SU5416 treatment (Fig. 3). The examination of histologic sections by independent observers indicated that tumor vessels were uniformly distributed throughout the tumors for both control and treated groups. No decrease in the number of vessels was observed after SU5416 treatment, and the aspect of the vessels remained the same, contrary to observations made after treatment with thalidomide (5). In conclusion, SU5416 did not induce any remodeling of tumor vasculature after 2 days of treatment.

Effect of SU5416 on the rate of oxygen consumption by tumor cells. The rate of oxygen consumption by TLT tumor cells excised from mice treated with SU5416 for 2 days was significantly reduced ($P < 0.0001$; Fig. 4). The mean slopes were 1.1 ± 0.03 μmol/L/min/2.10^7 cells/mL (n = 3) and −0.4 ± 0.02 μmol/L/min/2.10^7 cells/mL (n = 6) for control and SU5416 groups, respectively. This means that cells from SU5416-treated tumors consumed oxygen 2.8 times slower than control cells.

Effect of SU5416 on radiation sensitivity. To assess the therapeutic relevance of our finding (significant increase in tumor oxygenation), we combined SU5416 treatment (2 days) with 10-Gy radiotherapy. Figure 5*A* shows the tumor growth of TLT tumors that were injected with SU5416 or DMSO for 2 days, with or without irradiation 24 hours after the second injection. Without irradiation, SU5416 treatment did not affect tumor growth, as the time to reach 12 mm in size was 9.9 ± 1.7 days (n = 5) and 9.7 ± 0.8 days (n = 6) for the treated and control groups, respectively. When irradiated with 10 Gy (without SU5416 pretreatment), tumor growth was significantly delayed: the time to reach 12 mm was 14.8 ± 1.5 days (n = 5).

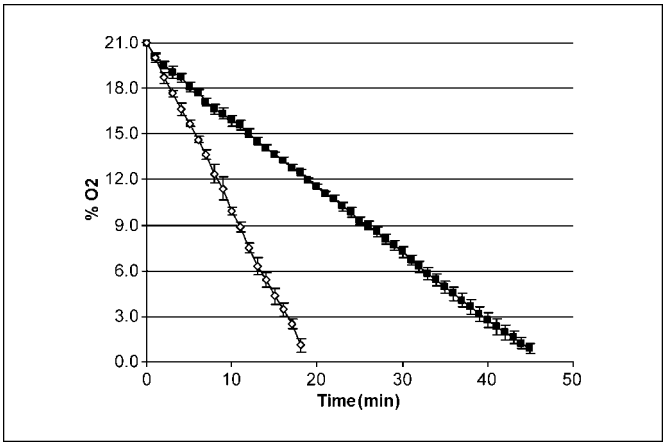

Figure 4. Effect of *in vivo* SU5416 treatment on rate of tumor cell oxygen consumption. ■, SU5416-treated group (n = 6); ◇, control group (n = 3). Treated tumors consumed oxygen 2.8 times slower than control cells. *Points,* percent O_2; *bars,* SE. ***, $P < 0.001$.

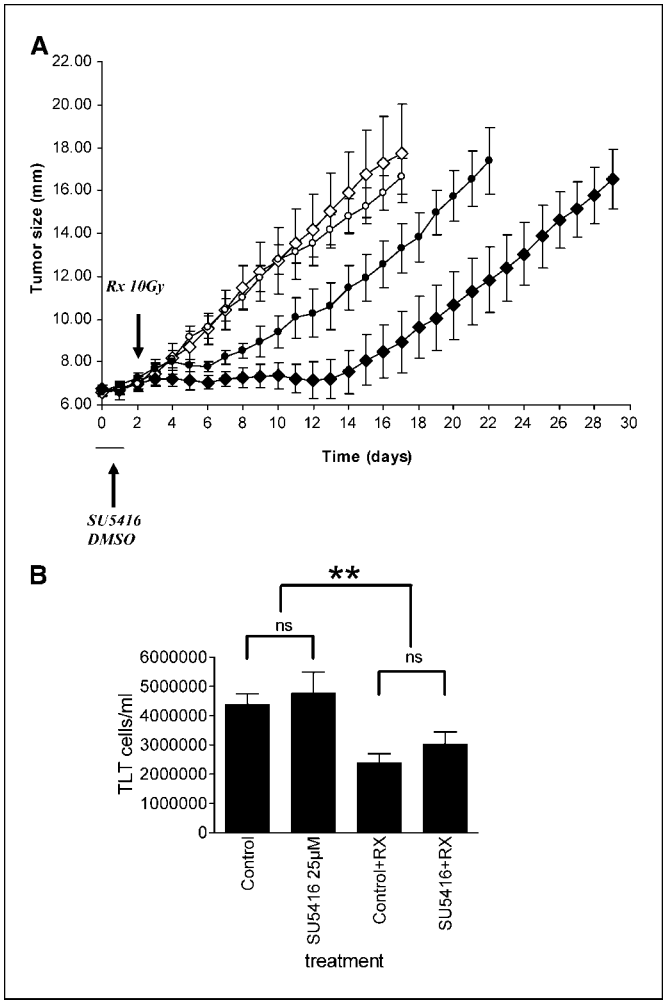

Figure 5. *A,* effect of the combination of SU5416 and radiation on TLT tumor regrowth. Mice were treated with SU5416 (◇; $n = 5$), DMSO (○; $n = 6$), 10 Gy of radiotherapy (*RX*) after 2 days of DMSO (●; $n = 5$), or with 10 Gy of radiotherapy after 2 days of SU5416 (◆; $n = 6$). Each point represents the mean tumor size ± SE. No difference in regrowth delay was observed between the control and the SU5416-treated groups (without irradiation). Delays in regrowth to 12 mm diameter were 14.8 ± 1.5 days for control plus radiotherapy (*control + RX*) and 21.90 ± 2.1 days for SU5416 plus radiotherapy (*SU5416 + RX; P* < 0.01). SU5416 increased the regrowth delay by a factor of 2.4. *B,* effect of SU5416 (25 μmol/L) on TLT cells evaluated by the trypan blue exclusion dye method. This technique showed an effect of the irradiation of 2 Gy on tumor cells. Nevertheless, SU5416 did not exert any cytotoxic or sensitizing effect. **, $P < 0.01$; *ns,* not significant.

Pretreatment with SU5416 before irradiation led to a significant increase in tumor growth delay (21.9 ± 2.1 days to reach 12 mm; $n = 6$). To discriminate between an oxygen effect and a direct radiosensitizing effect, radiosensitivity was tested on TLT cells irradiated in the presence of SU5416 (Fig. 5*B*). A 2-Gy dose was used as it is the dose, which induces ~50% tumor cells death. Compared with control cells, SU5416 did not exert any sensitizing effect. Meanwhile, 2-Gy irradiation led to a significant decrease in tumor cell number for both experiments ($P < 0.01$). These observations show that SU5416 radiosensitizes tumors through changes in the tumor oxygenation rather than by a direct sensitizing effect.

Effect of SU5416 on chemotherapeutic treatment. To evaluate the possible adjuvant effect of SU5416 on chemotherapy, we carried out a protocol that used a suboptimal dose of cyclophosphamide to facilitate the identification of a possible potentiation of combined treatments. This protocol has already been used to show the benefits of drugs that transiently open the tumor vascular bed (5, 21). Results are shown in Fig. 6. There was no significant difference in tumor growth between the groups receiving SU5416, DMSO, the combination SU5416 plus cyclophosphamide, or the combination DMSO plus cyclophosphamide. This indicates that SU5416 pretreatment did not potentiate the effects of chemotherapy.

Discussion

The major findings of the present study are the following: (*a*) SU5416, a specific VEGFR antagonist, is unable to induce a "normalization" of tumor vasculature in the tumor models studied, contrary to other antiangiogenic agents; (*b*) SU5416 induces tumor reoxygenation by a long-term effect on the oxygen consumption of the tumor cells; and (*c*) SU5416 potentiates the effects of radiotherapy but not of cyclophosphamide, results that are consistent with the effects observed in the tumor microenvironment.

Complex events occurring in the tumor microenvironment after treatment with SU5416. Several years ago, when preclinical studies with antiangiogenic agents started, it was believed that these agents should lead to a decrease in tumor perfusion and delivery of endogenous and exogenous compounds. This is still the targeted end-point of antiangiogenic therapy, and the noninvasive biomarkers for assessing therapeutic response are based on perfusion measurements (22). As already emphasized, however, the dynamic evolution of tumor blood supply is more complex than previously thought, and recent preclinical studies (4–11) have shown a transient increase in tumor blood flow early after treatment with several antiangiogenic agents (transient normalization of the tumor vasculature). A key issue is to know whether this phenomenon occurs with all antiangiogenic agents. Our results indicate that SU5416 is clearly distinguishable from other antiangiogenic agents (such as thalidomide), as we did not observe any remodeling of the tumor vasculature (Fig. 3) or any

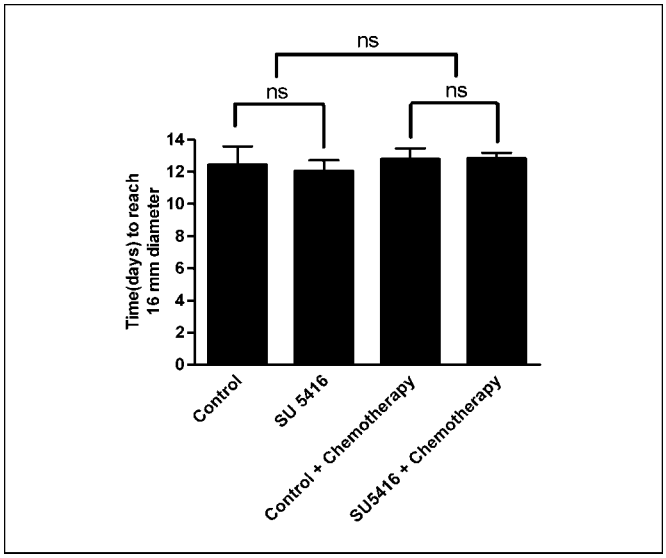

Figure 6. Effect of the combination of SU5416 and suboptimal dose chemotherapy on TLT tumor regrowth. Note that the time for tumors to double size (to reach 16 mm in diameter) was the same whatever treatment or treatment combination was used. *ns,* not significant.

change in tumor hemodynamic variables (Fig. 2). How can we explain the absence of the "normalization" phase in the present study? One possible explanation is that when the VEGF/VEGFR system is blocked, another angiogenic pathway, including bFGF, platelet-derived growth factor, transforming growth factor-β, and Tie-2 signaling may compensate for it (13). The fact that thalidomide was able to induce a transient normalization of tumor vasculature in the same tumor model is consistent with this hypothesis, as thalidomide acts on different angiogenic pathways (5). The action of SU5416 on the tumor vasculature could also be dependent on the proliferation rate of the tumor model used and the duration of the treatment. This normalization process following SU5416 treatment has been observed in slowly growing tumors, such as mammary tumors inoculated into the liver of rats treated for 14 days (23). In our study, TLT and FSAII tumors are highly proliferative models, in which the inhibitory effects of SU5416 could be suppressed by the rapid turn over of Flk-1.

Another important finding observed in our study is that reoxygenation of the tumor occurred even without normalization of the tumor vasculature. It should be emphasized that this finding was made possible only by using multiple modalities to characterize the tumor evolution of the tumor microenvironment. We clearly show that this effect was mediated by inhibition of tumor cell oxygen consumption (Fig. 4). Other less invasive methods, such as microelectrodes (24) and near-IR spectroscopy (25), could also be used to assess the tumor oxygen consumption. The reduction in oxygen consumption by a factor of 2.8 observed in the present study is sufficient to abolish tumor hypoxia as has been observed using other treatments (20, 26). It has also been shown that modification of oxygen consumption is much more efficient at alleviating hypoxia than modification of oxygen delivery (27). To our knowledge, this is the first example of a modulator of tumor oxygen consumption that has a long-term effect. Thus far, only acute effects on mitochondrial respiration have been reported [e.g., using meta-iodobenzylguanidine (28), insulin (20), and anti-inflammatory agents (26)]. This long-term effect on tumor oxygen consumption may represent a novel target for this class of agents (analogues of SU5416), which could be exploited in combined therapies.

Relevance for combined therapies. Before combining different treatment modalities, it is crucial to study the effect of the first treatment on the tumor oxygenation to determine the best time schedule for administration (5, 12). Combination studies using SU5416 together with radiotherapy have already been conducted (29–31), but none have studied the dynamic evolution of tumor variables to propose a rational administration schedule. Our results clearly show that SU5416 induced reoxygenation of the TLT tumor despite the absence of an effect on tumor perfusion. These results are remarkable in the sense that they clearly predict the effects of combined therapies on tumor growth. A clear benefit was observed when combining irradiation with SU5416 treatment. As there was no direct radiosensitizing effect of SU5416 on the tumor cells, the increase in the efficacy of radiotherapy is clearly due to the effect on tumor oxygenation. However, this effect could be reduced for well-oxygenated tumors compared with TLT as oxic cells are known to present a better radiosensitivity. Meanwhile, each tumor, even the well-oxygenated ones, contains hypoxic regions, which could benefit from this phenomenon of reoxygenation and therefore induced radiosensitization. We found previously that the magnitude of the increase in tumor oxygenation (twice increase) was sufficient to enhance the response of tumors to radiation therapy (5, 26). By contrast, SU5416 did not lead to any benefit when combined with a suboptimal dose of cyclophosphamide. We ascribe this lack of a synergistic effect to the absence of an effect on perfusion as there was no normalization of the tumor vasculature. Therefore, the same result could be expected for therapeutic doses. Moreover, using the same protocol, we found previously a therapeutic benefit when combining cyclophosphamide and thalidomide during the "normalization" window. We may also ask whether oxygen could play a role in the sensitivity of tumors to cyclophosphamide? Several previous chemotherapy studies have shown that oxygen can indeed, albeit in an indirect manner, modulate the efficacy of chemotherapy. Consequently of a decline in nutrient and oxygen availability, cells further away from the vascular system may divide at a reduced rate and thus be protected from the effects of chemotherapeutic agents whose activity is selective for rapidly dividing cell populations. Consequently, the increase in oxygen availability could potentially improve the cytotoxic effect of a chemotherapeutic drug. Our results here clearly indicate that this was not the case when using cyclophosphamide in this tumor model.

Conclusion

The evolution of the tumor oxygenation after antiangiogenic therapy is complex and strongly depends on the type of drug, the duration of treatment, and the tumor being investigated. Apart from "normalization" of the tumor vasculature, an effect on tumor oxygen consumption could also explain the synergistic effect when combining radiotherapy with antiangiogenic treatments. The dynamic study of changes in the tumor oxygenation during antiangiogenic treatment is of crucial importance for planning how best to combine such drugs with radiotherapy and chemotherapy. Clearly, there is a need to tailor treatments on an individual basis. The optimization of treatment schedules in patients will benefit from recent developments in spectroscopy/imaging technologies, such as EPR (32), MRI (22), and positron emission tomography (33).

Acknowledgments

Received 5/22/2006; revised 7/25/2006; accepted 8/8/2006.

Grant support: Belgian FNRS grant 7.4503.02, the Fonds Joseph Maisin, and the "Actions de Recherches Concertées-Communauté française de Belgique 04/09-317."

The costs of publication of this article were defrayed in part by the payment of page charges. This article must therefore be hereby marked *advertisement* in accordance with 18 U.S.C. Section 1734 solely to indicate this fact.

We thank Guerbet Laboratories (Roissy, France) for providing P792.

References

1. Jain RK. Normalisation of tumor vasculature: an emerging concept in antiangiogenic therapy [review]. Science 2005;307:58–62.
2. Folkman J. Role of angiogenesis in tumor growth and metastasis [review]. Semin Oncol 2002;29:15–8.
3. Carmeliet P, Jain RK. Angiogenesis in cancer and other diseases [review]. Nature 2000;407:249–57.
4. Winkler F, Kozin SV, Tong RT, et al. Kinetics of vascular normalization by VEGFR2 blockade governs brain tumor response to radiation: role of oxygenation, angiopoietin-1, and matrix metalloproteinases. Cancer Cell 2004;6:553–63.
5. Ansiaux R, Baudelet C, Jordan BF, et al. Thalidomide radiosensitizes tumors through early changes in the tumor microenvironment. Clin Cancer Res 2005;11:743–50.
6. Huber PE, Bischof M, Jenne J, et al. Trimodal cancer treatment: beneficial effects of combined antiangiogenesis, radiation, and chemotherapy. Cancer Res 2005;65:3643–55.

7. Salnikov AV, Roswall P, Sundberg C, Gardner H, Heldin NE, Rubin K. Inhibition of TGF-β modulates macrophages and vessel maturation in parallel to a lowering of interstitial fluid pressure in experimental carcinoma. Lab Invest 2005;85:512–21.

8. Tong RT, Boucher Y, Kozin SV, Winkler F, Hicklin DJ, Jain RK. Vascular normalization by vascular endothelial growth factor receptor 2 blockade induces a pressure gradient across the vasculature and improves drug penetration in tumors. Cancer Res 2004;64:3731–6.

9. Vosseler S, Mirancea N, Bohlen P, Mueller MM, Fusenig NE. Angiogenesis inhibition by vascular endothelial growth factor receptor-2 blockade reduces stromal matrix metalloproteinase expression, normalizes stromal tissue, and reverts epithelial tumor phenotype in surface heterotransplants. Cancer Res 2005;65:1294–305.

10. Wildiers H, Guetens G, De Boek G, et al. Effect of antivascular endothelial growth factor treatment on the intratumoral uptake of CPT-11. Br J Cancer 2003; 88:1979–86.

11. Segers J, Fazio VD, Ansiaux R, et al. Potentiation of cyclophosphamide chemotherapy using the anti-angiogenic drug thalidomide: Importance of optimal scheduling to exploit the "normalization" window of the tumor vasculature. Cancer Lett. Epub 2006 Jan 17.

12. Jain RK. Normalizing tumor vasculature with anti-angiogenic therapy: a new paradigm for combination therapy [review]. Nat Med 2001;7:987–9.

13. Takamoto T, Sasaki M, Kuno T, Tamaki N. Flk-1 specific kinase inhibitor (SU5416) inhibited the growth of GS-9L glioma in rat brain and prolonged the survival Kobe. J Med Sci 2001;47:181–91.

14. Fong TA, Shawver LK, Sun L, et al. SU5416 is apotent and selective inhibitor of the vascular endothelial growth factor receptor (FLK-1/KDR) that inhibits tyrosine kinase catalysis, tumor vascularization, and growth of multiple tumor types. Cancer Res 1999;59:99–106.

15. Taper HS, Woolley GW, Teller MN, Lardis MP. A new transplantable mouse liver tumor of spontaneous origin. Cancer Res 1966;26:143–8.

16. Volpe JP, Hunter N, Basic I, Milas L. Metastatic properties of murine sarcomas and carcinomas. I. Positive correlation with lung colonization and lack of correlation with s.c. tumor take. Clin Exp Metastasis 1985;3:281–94.

17. Gallez BF, Jordan B, Baudelet C, Misson PD. Pharmacological modifications of the partial pressure of oxygen in tumors. Evaluation using *in vivo* EPR oximetry. Magn Reson Med 1999;42:627–30.

18. Baudelet C, Ansiaux R, Jordan BF, Havaux X, Macq B, Gallez B. Physiological noise in murine solid tumor using T2*-weighted gradient-echo imaging: a marker of tumour acute hypoxia? Phys Med Biol 2004;49: 3389–411.

19. Galbraith SM, Maxwell RJ, Lodge MA, et al. Combrestatin A4 phosphate has tumor antivascular activity in rat and man as demonstrated by dynamic magnetic resonance imaging. J Clin Oncol 2003;21:2831–42.

20. Jordan BF, Gregoire V, Demeure RJ, et al. Insulin increases the sensitivity of tumors to irradiation: involvement of an increase in tumor oxygenation mediated by a nitric oxide-dependent decrease of the tumor cells oxygen consumption. Cancer Res 2002;62: 3555–61.

21. Ansiaux R, Baudelet C, Cron GO, et al. Botulinum toxin potentiates cancer radiotherapy and chemotherapy. Clin Cancer Res 2006;12:1276–83.

22. Padhani AR, Leach MO. Antivascular cancer treatments: functional assessments by dynamic contrast-enhanced magnetic resonance imaging [review]. Abdom Imaging 2005;30:324–41.

23. Kan Z, Phongkitkarun S, Kobayashi S, et al. Functional CT for quantifying tumor perfusion in antiangiogenic therapy in rat model. Radiology 2005; 237:151–8.

24. Dewhirst MW, Secomb TW, Ong ET, Hsu R, Gross JF. Determination of local oxygen consumption rates in tumors. Cancer Res 1994;54:3333–6.

25. Song Y, Kim JG, Mason RP, Liu H. Investigation of rat breast tumour oxygen consumption by near-infrared spectroscopy. J Phys D: Appl Phys 2005;38: 2682–90.

26. Crokart N, Radermacher K, Jordan BF, et al. Tumor radiosensitization by antiinflammatory drugs: evidence for a new mechanism involving the oxygen effect. Cancer Res 2005;65:7911–6.

27. Secomb TW, Hsu R, Ong ET, Gross JF, Dewhirst MW. Analysis of the effects of oxygen supply and demand on hypoxic fraction in tumors. Acta Oncol 1995;34:313–6.

28. Biaglow JE, Manevich Y, Leeper D, et al. MIBG inhibits respiration: potential for radio- and hyperthermic sensitization. Int J Radiat Oncol Biol Phys 1998;42: 871–6.

29. Ning S, Laird D, Cherrington JM, Knox SJ. The antiangiogenic agents SU5416 and SU6668 increase the antitumor effects of fractionated irradiation. Radiat Res 2002;157:45–51.

30. Geng L, Donnelly E, McMahon G, et al. Inhibition of vascular endothelial growth factor receptor signaling leads to reversal of tumor resistance to radiotherapy. Cancer Res 2001;61:2413–9.

31. Schuuring J, Bussink J, Bernsen HJ, Peeters W, van Der Kogel AJ. Irradiation combined with SU5416: microvascular changes and growth delay in a human xenograft glioblastoma tumor line. Int J Radiat Oncol Biol Phys 2005;61:529–34.

32. Swartz HM, Khan N, Buckey J, et al. Clinical applications of EPR: overview and perspectives. NMR Biomed 2004;17:335–51.

33. Rajendran JG, Krohn KA. Imaging hypoxia and angiogenesis in tumors. Radiol Clin North Am 2005;43: 169–87.